

## Supporting Information

### Magnetic anisotropy and structural flexibility in the field-induced single ion magnets $[\text{Co}\{(\text{OPPh}_2)(\text{EPPh}_2)\text{N}\}_2]$ , E = S, Se, explored by experimental and computational methods

Eleftherios Ferentinos,<sup>a</sup> Demeter Tzeli,<sup>b,c</sup> Silvia Sottini,<sup>d</sup> Edgar J. J. Groenen,<sup>d</sup> Mykhaylo Ozerov,<sup>e</sup> Giordano Poneti,<sup>\*f</sup> Kinga Kaniewska-Laskowska,<sup>g</sup> J. Krzystek,<sup>\*e</sup> Panayotis Kyritsis<sup>\*a</sup>

<sup>a</sup>Inorganic Chemistry Laboratory, Department of Chemistry, National and Kapodistrian University of Athens, Panepistimiopolis, GR-15771 Athens, Greece.

<sup>b</sup>Physical Chemistry Laboratory, Department of Chemistry, National and Kapodistrian University of Athens, Panepistimiopolis, GR-15771 Athens, Greece.

<sup>c</sup>Theoretical and Physical Chemistry Institute, National Hellenic Research Foundation, 48 Vassileos Constantinou Ave., GR-11635 Athens, Greece

<sup>d</sup>Huygens-Kamerlingh Onnes Laboratory, Department of Physics, Leiden University, Niels Bohrweg 2, 2333 CA Leiden, The Netherlands

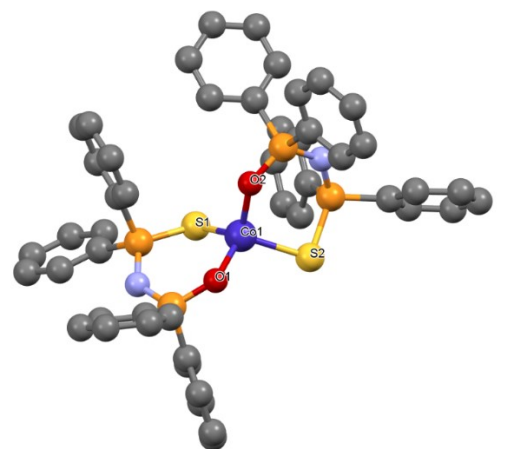
<sup>e</sup>National High Magnetic Field Laboratory, Florida State University, Tallahassee, Florida 32310, United States.

<sup>f</sup>Instituto de Química, Universidade Federal do Rio de Janeiro, 21941-909 Rio de Janeiro, Brazil

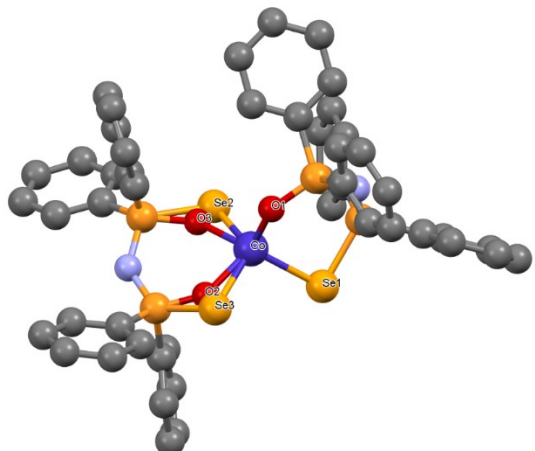
<sup>g</sup>Department of Inorganic Chemistry, Faculty of Chemistry, Gdańsk University of Technology, G. Narutowicza St. 11/12, Gdańsk PL-80-233, Poland.

<b>Contents</b>	<b>Page</b>
X-ray crystallography	3
DC Magnetometry	4-5
FIRMS / HFEPR	6-8
High-resolution multifrequency EPR	9-10
AC Magnetometry	11-12
Computational studies	13-24
References	24

## X-ray crystallography



(a)



(b)

**Figure S1.** Crystal structure of (a)  $\text{CoO}_2\text{S}_2$ <sup>1</sup> and (b)  $\text{CoO}_2\text{Se}_2$ .<sup>2</sup> Color coding: Co (blue), O (red), S (yellow), Se (darker brown), P (brown), N (light blue), C (gray). The observed structural disorder of  $\text{CoO}_2\text{Se}_2$  is shown.

## DC Magnetometry

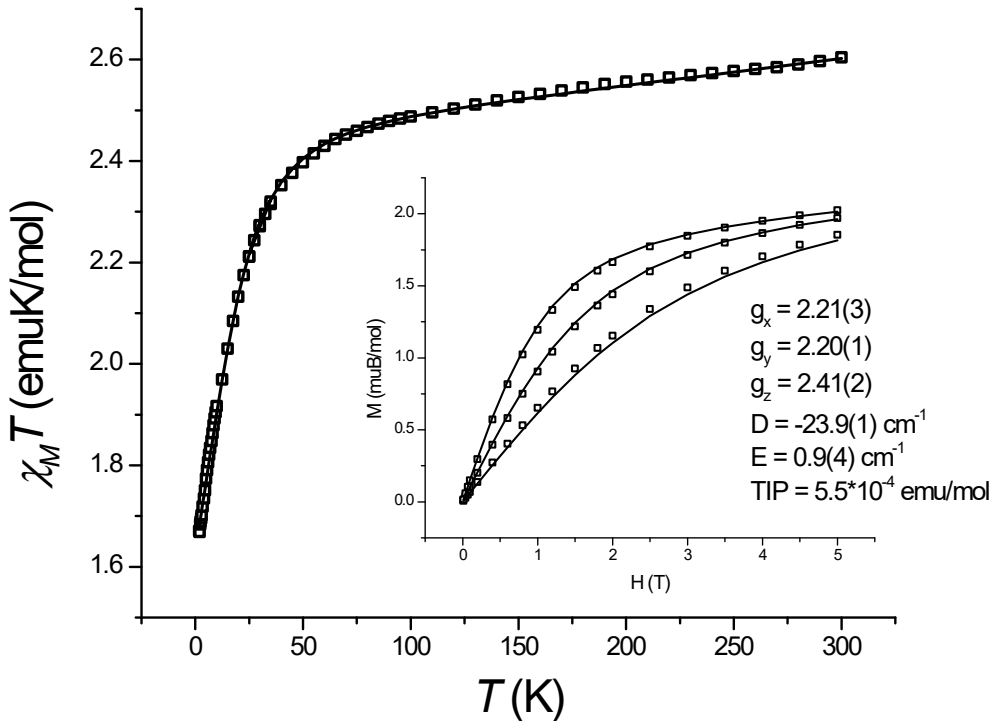
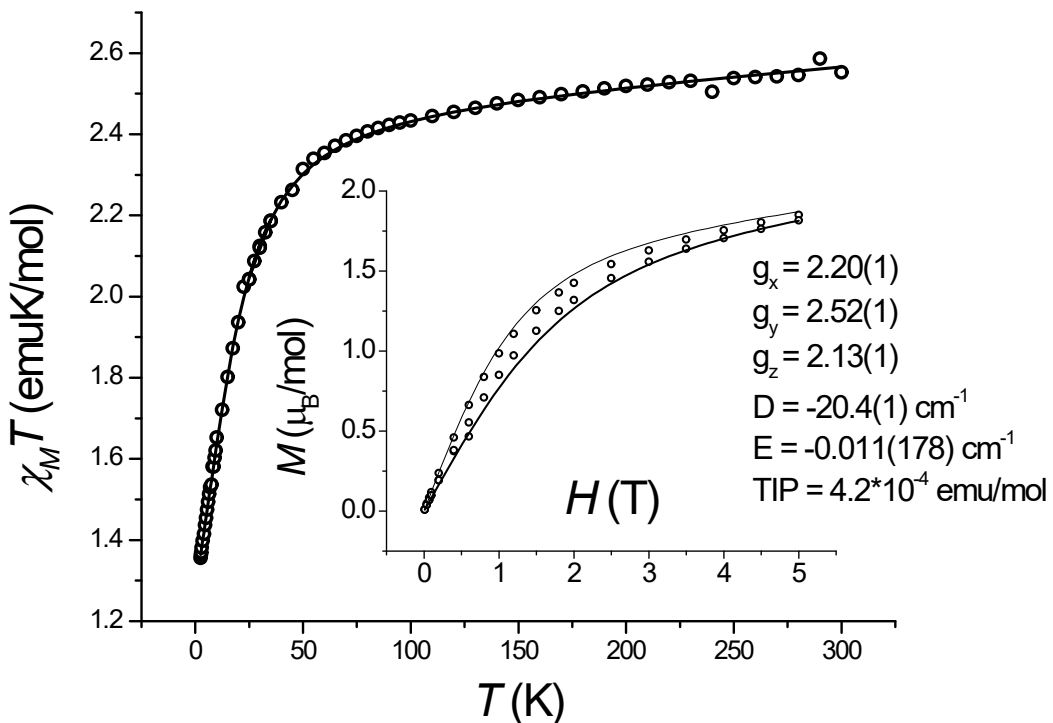


**Figure S2.** Temperature dependence of the  $\chi_M T$  product (main panel) and isothermal magnetizations of  $\text{CoO}_2\text{S}_2$  (empty circles), along with the best fitting lines calculated as described in the text.



## FIRMS / HFEPR

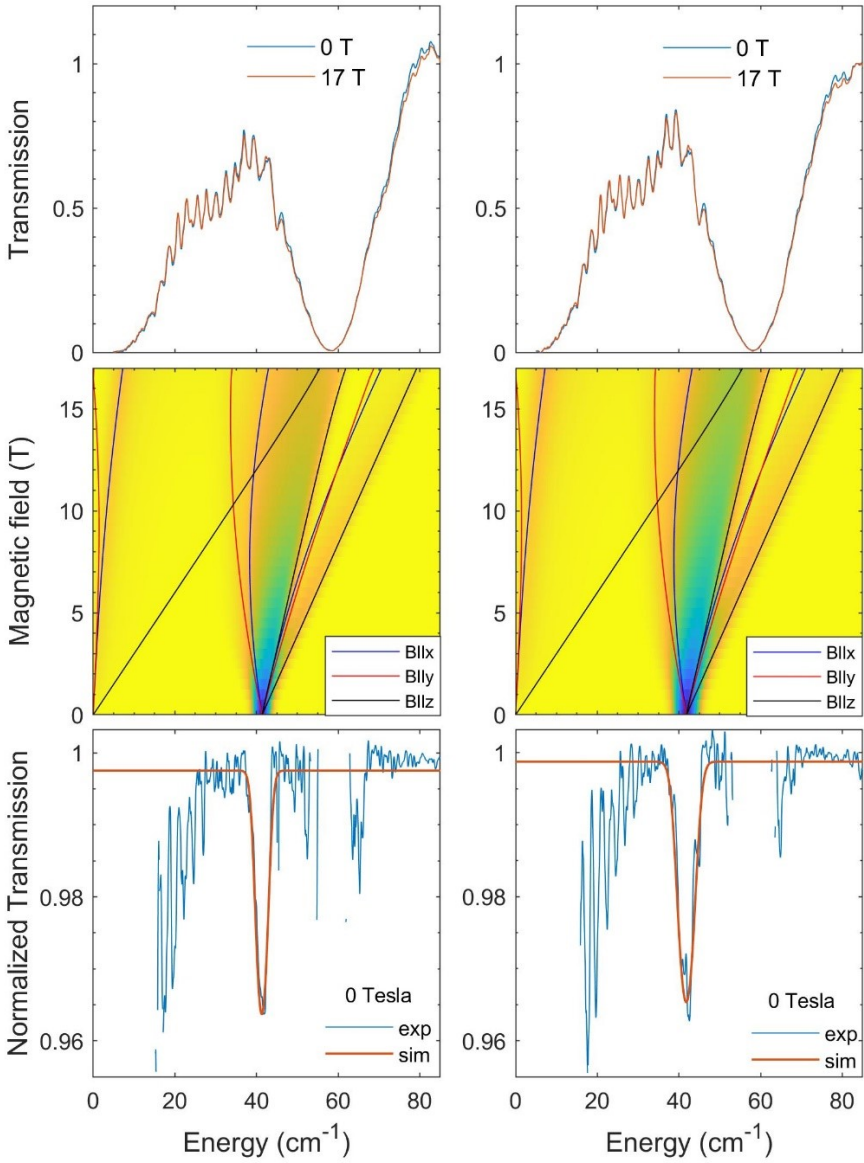


**Figure S4.** Additional FIRMS data for  $\text{CoO}_2\text{E}_2$  complexes:  $\text{E} = \text{S}$  (left) and  $\text{E} = \text{Se}$  (right). The top panel shows the transmission signal (single beam) measured at 0 and 17 T. The intensity drops between  $55$  and  $65 \text{ cm}^{-1}$ , as well as the oscillation pattern is caused by instrumental response of the experimental set-up. The middle panel shows the 2D intensity map of the magnetic resonance absorption calculated for the powder sample using  $S = 3/2$  Hamiltonian model and parameters listed in Table 2 of the main text. The solid lines are the same as in Figure 2 and indicate transition energies for magnetic fields applied along x, y, and z directions of the zfs tensor. The bottom panel compares the zero-field spectra taken from experimental (Figure 2) and simulated (middle panel) 2D color maps. The Easy-Spin software<sup>3</sup> was employed for the analysis of the FIRMS data

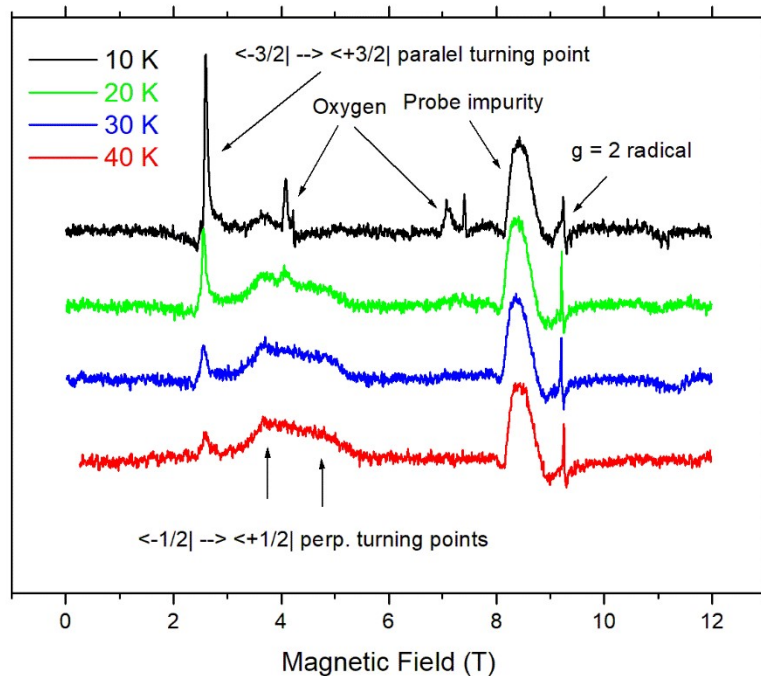


**Figure S5.** HFEPR spectra of  $\text{CoO}_2\text{Se}_2$  at various temperatures. Transitions within both the  $M_s = \pm 3/2$  and  $M_s = \pm 1/2$  Kramers doublets are observable. The former gets weaker with increasing temperature while the latter gets stronger, which means the former is the ground state.

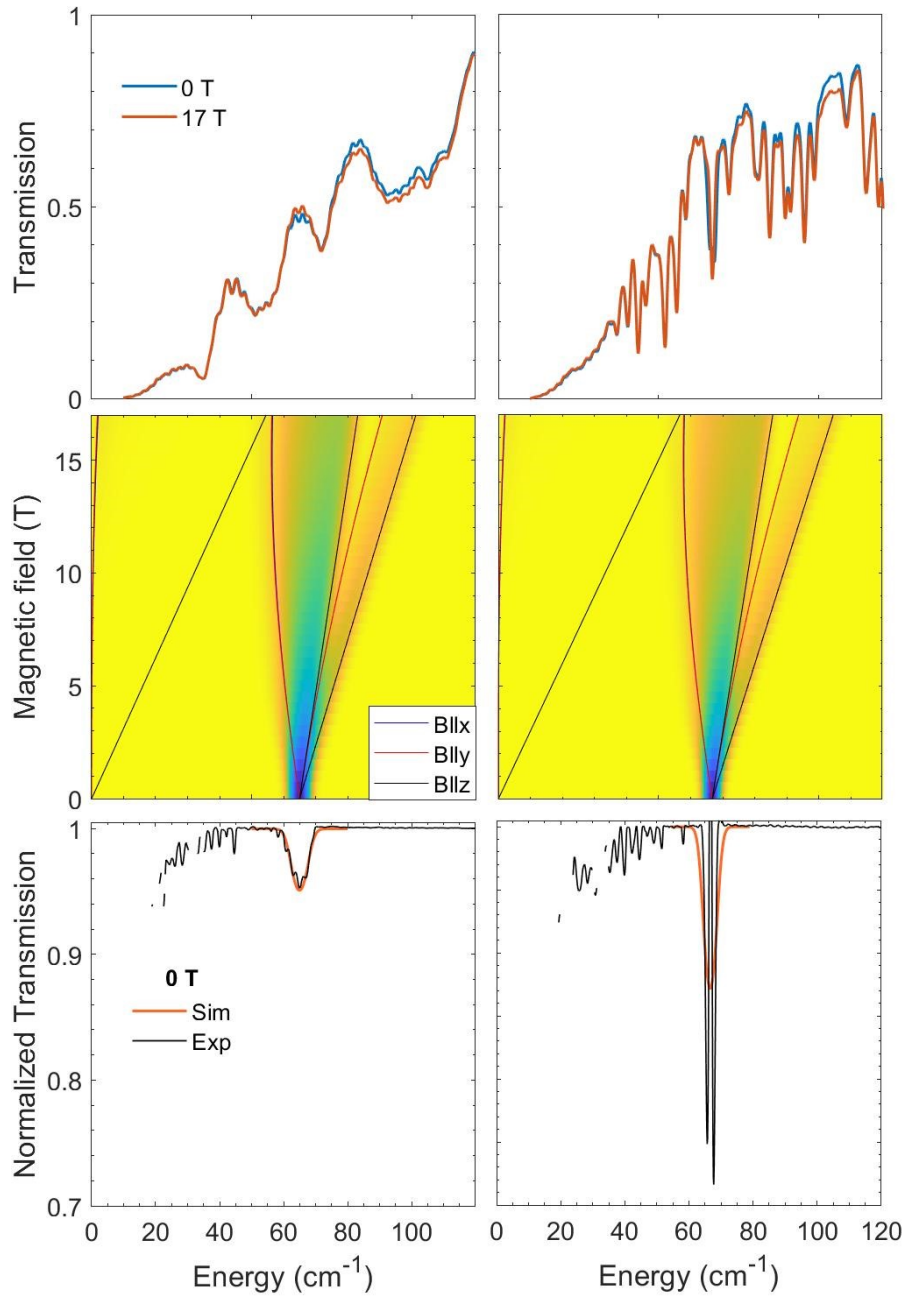


**Figure S6.** Additional FIRMS data for  $\text{CoE}_4$  complexes:  $E = \text{S}$  (left) and  $E = \text{Se}$  (right.). The top panel shows the transmission signal (single beam) measured at 0 and 17 T. The middle panel shows the 2D intensity map of the magnetic resonance absorption calculated for the powder sample using  $S = 3/2$  Hamiltonian model and parameters mentioned in the main text. The solid lines are same as in the Figure 3 and indicate transition energies for magnetic fields applied along x, y, and z directions of the zfs tensor. The bottom panel compares the zero-field spectra taken from experimental (Figure 3) and simulated (middle panel) 2D color maps. Two narrow peaks in  $\text{CoSe}_4$  evidence the hybridized ground state due to the spin-phonon coupling with a vibrational mode at  $66.7 \text{ cm}^{-1}$ . In high magnetic fields the magnetic transition is shifted away, and the vibrational mode restores single-peak lineshape (red curve in top panel). The Easy-Spin software<sup>3</sup> was employed for the analysis of the FIRMS data.

## High-resolution multifrequency EPR

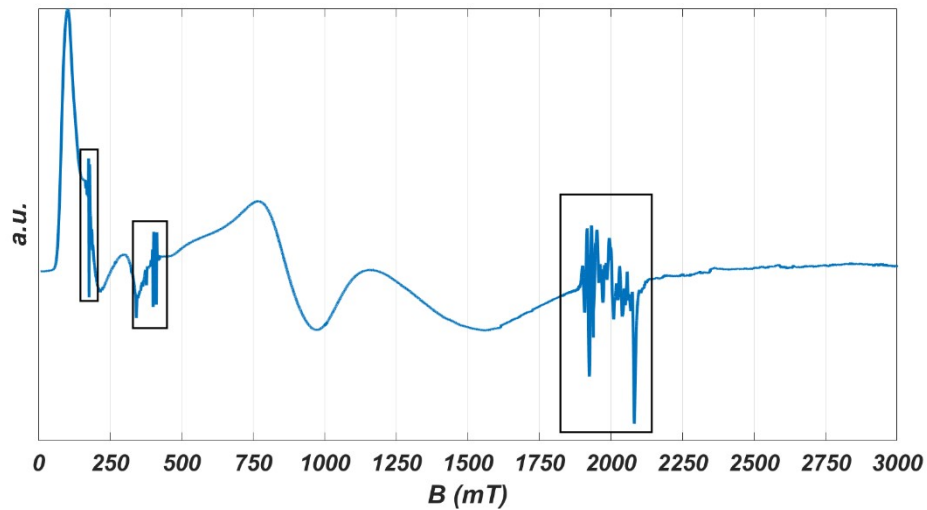


**Figure S7.** The EPR spectrum of a powder sample of  $\text{CoO}_2\text{S}_2$  at 9 GHz and 5 K. The sharp signals in the black boxes are background signals from the microwave cavity.

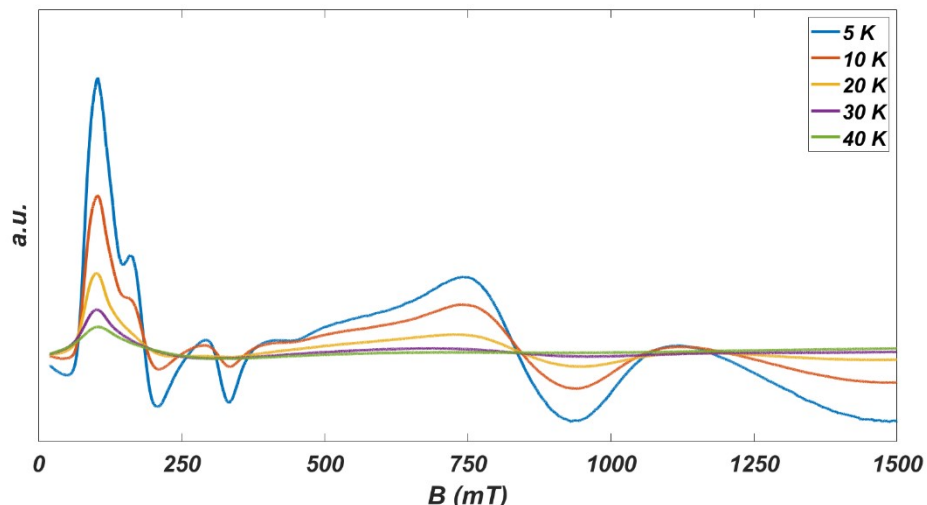


**Figure S8.** The variation of the EPR spectrum at 9 GHz of a powder sample of  $\text{CoO}_2\text{S}_2$  as a function of temperature.

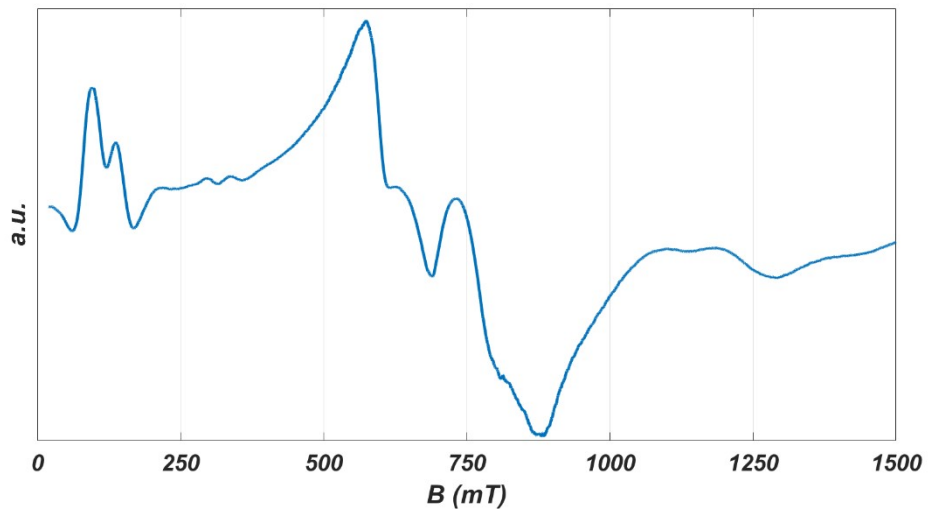


**Figure S9.** The EPR spectrum of a powder sample of  $\text{CoO}_2\text{Se}_2$  at 9 GHz and 5 K.

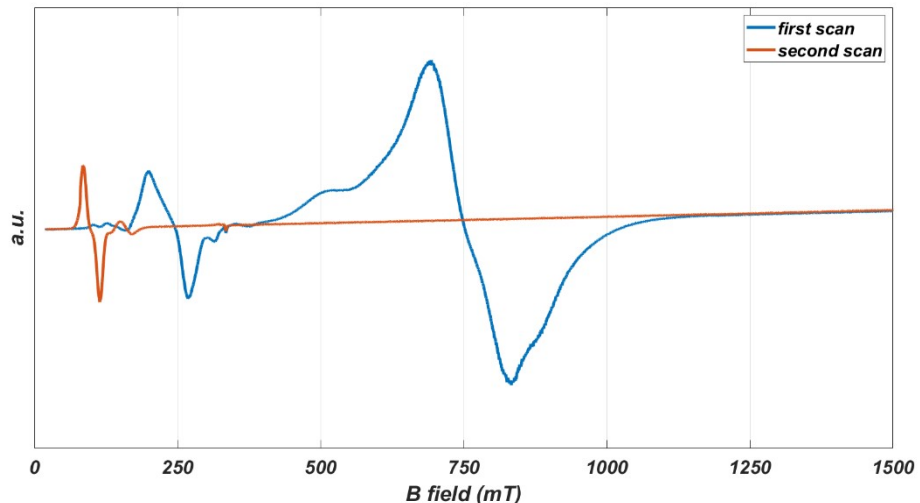


**Figure S10.** Two subsequent scans of the EPR spectrum at 9 GHz and 5 K of a single crystal of  $\text{CoO}_2\text{Se}_2$ , on purpose left free to move in the EPR tube. The first scan represents the spectrum for an arbitrary orientation of the magnetic field with respect to the crystal and shows distinct contributions of the two magnetically inequivalent molecules in the unit cell. The second scan has been taken after self-orientation of the crystal in a field of 1.5 T. For this orientation of the magnetic field with respect to the crystal, the molecules have become magnetically equivalent and their EPR signals coincide.

## AC Magnetometry

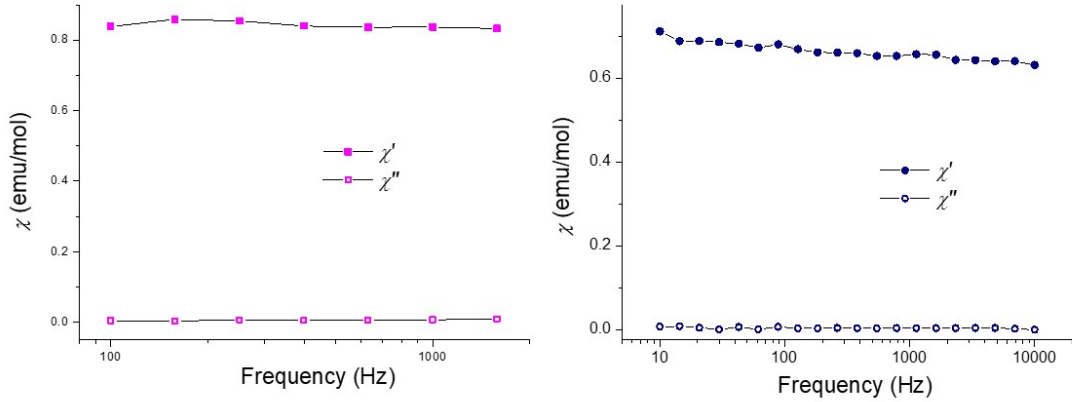


**Figure S11.** Temperature dependence of the magnetic susceptibility of  $\text{CoO}_2\text{S}_2$  (left panel) and  $\text{CoO}_2\text{Se}_2$  (right panel) measured with no static applied field at 1.9 K.

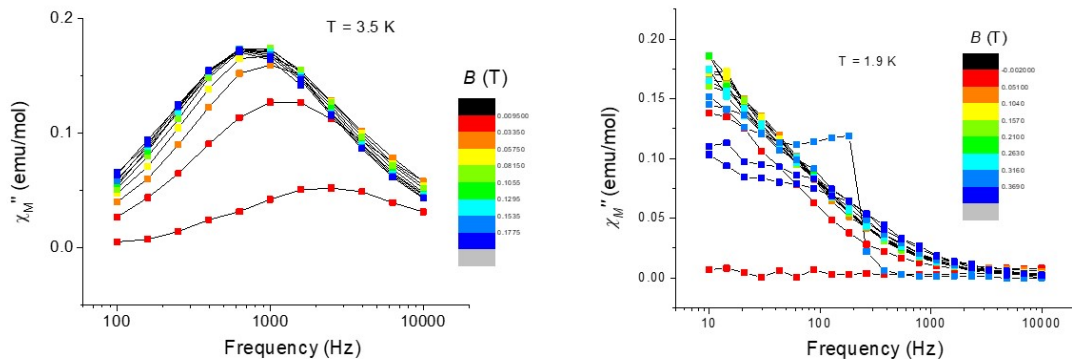


**Figure S12.** Isothermal frequency dependence of the out-of-phase magnetic susceptibility of  $\text{CoO}_2\text{S}_2$  (left panel) and  $\text{CoO}_2\text{Se}_2$  (right panel) measured with different static magnetic fields applied.

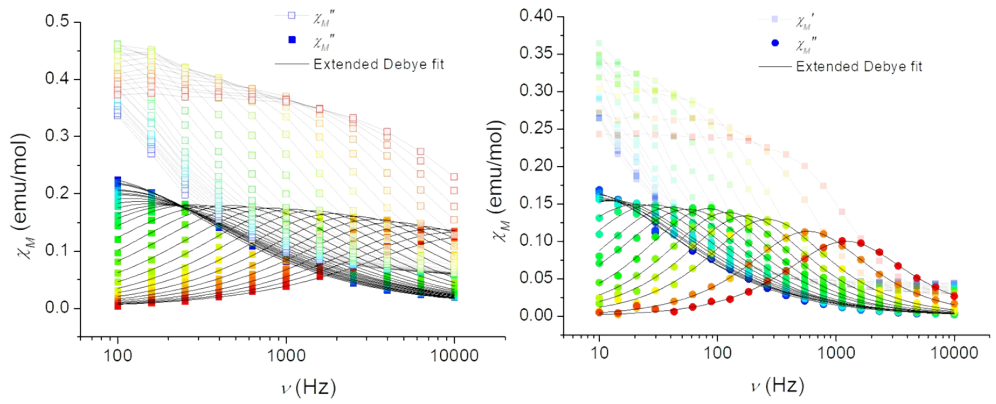


**Figure S13.** Frequency dependence of the molar in-phase ( $\chi_M'$ ) and out-of-phase ( $\chi_M''$ ) magnetic susceptibility of  $\text{CoO}_2\text{S}_2$  (left) and  $\text{CoO}_2\text{Se}_2$  (right), measured with a 120 mT static field applied. The best fitting functions arising from the use of the extended Debye model are reported as black lines.

## **Computational studies**

### **Computational study of the $\text{CoO}_2\text{E}_2$ , $\text{E} = \text{S, Se}$ complexes**

The seven lowest in energy states for both complexes are quartet states. The vertical transition energies from the ground state to the six lowest excited states are less than 0.8 eV. Depending on the geometry, the leading electronic configuration of these states differs (Table S3 of SI). Additionally, it is found that  $\text{CoO}_2\text{S}_2$  is more multireference than  $\text{CoO}_2\text{Se}_2$ . Furthermore, the energetically optimized geometry for the (b) structure of  $\text{CoO}_2\text{Se}_2$  has a significant smaller multireference character, i.e., the coefficient of the leading configuration state function is 0.86 contrary to 0.55 for the corresponding experimental crystal structure, or 0.47 for the crystal structure of  $\text{CoO}_2\text{S}_2$ .

The NEVPT2 vertical transition energies are depicted in Figure S14. It is found that in all cases the shape of the energetic diagram is similar, where four groups of states are formed (Figure S14). Furthermore, the inclusion of the LFT approach on NEVPT2 results in a more condensed energy diagram within each group of states than NEVPT2 energy diagram for all structures (Figure S14), while the gap between the groups is increased using the NEVPT2-LFT method compared to NEVPT2. The three gaps are of 1.3 (1.4 LFT) eV, 0.9 (1.1 LFT) and 2.2 (2.4 LFT) eV. Finally, the lowest in energy doublet state is located among the lowest in energy states of the second group of states, i.e. about ~1.3 (1.4 LFT) eV.

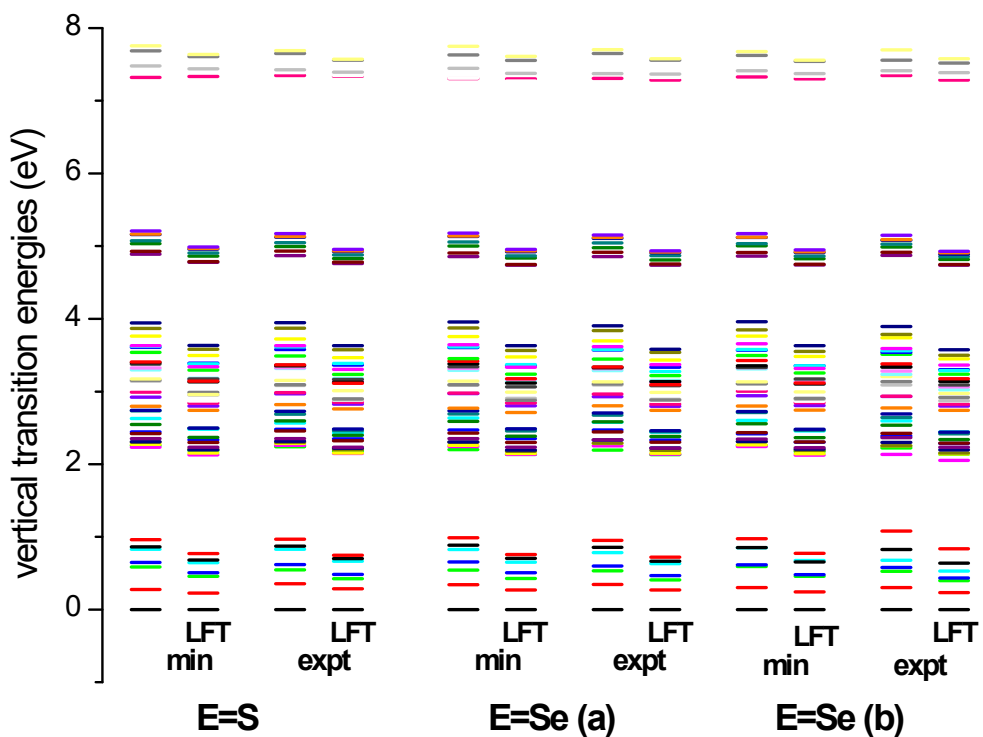


**Figure S14.** NEVPT2 and NEVPT2-LFT vertical transition energies of the calculated structures at the minimum energy structures and at the geometry of the experimental crystal structure of  $\text{CoO}_2\text{E}_2$ ,  $\text{E} = \text{S}, \text{Se}$ .

**Table S1.** Selected geometries of  $\text{CoO}_2\text{E}_2$ , E = S, Se complexes, bond distances in Å, angles and dihedral angles in degrees (°).

<b>E atom</b>	<b>Geom</b>	<b>Co–O</b>	<b>Co–E</b>	<b>Co–O'</b>	<b>Co–E'</b>		
<b>S</b>	Opt <sup>b</sup>	1.953	2.384	1.957	2.371		
	Opt <sup>c</sup>	1.972	2.394	1.966	2.404		
	Expt	1.956	2.343	2.003	2.320		
<b>Se(a)</b>	Opt <sup>b</sup>	1.960	2.428	1.941	2.430		
	Opt <sup>c</sup>	1.966	2.515	1.975	2.503		
	Expt	1.970	2.431	1.952	2.457		
<b>Se(b)</b>	Opt <sup>a</sup>	1.958	2.433	1.955	2.439		
	Expt	1.952	2.457	2.126	2.377		
<hr/>							
<b>E</b>	<b>Geom</b>	<b>E'CoO</b>	<b>E'CoO'</b>	<b>OCoO'</b>	<b>SCoS'</b>	<b>NCoN'</b>	
<b>S</b>	Opt <sup>b</sup>	104.50	104.40	108.71	112.92	163.58	
	Opt <sup>c</sup>	104.20	104.63	109.78	112.46	162.97	
	Expt	105.96	110.34	105.85	109.09	161.06	
<b>Se(a)</b>	Opt <sup>b</sup>	109.02	107.33	112.44	114.84	169.55	
	Opt <sup>c</sup>	105.29	104.61	108.93	111.81	159.75	
	Expt	108.50	106.15	108.00	107.18	159.31	
<b>Se(b)</b>	Opt <sup>a</sup>	106.80	107.64	107.96	112.68	165.45	
	Expt	106.15	106.75	117.59	104.20	159.31	
<hr/>							
<b>E</b>	<b>Geom</b>	<b>PSOP</b>	<b>P'S'O'P'</b>	<b>OCoSS'</b>	<b>OCoS'O'</b>	<b>O'CoS'S</b>	<b>O'CoS'O</b>
<b>S</b>	Opt <sup>b</sup>	38.46	-38.60	126.67	-116.79	120.12	-119.46
	Opt <sup>c</sup>	39.11	-39.02	119.70	-120.41	125.93	-118.10
	Expt	16.65	-31.94	124.37	-114.20	121.50	-119.64
<b>Se(a)</b>	Opt <sup>b</sup>	40.90	-35.71	-115.49	123.54	-122.27	119.06
	Opt <sup>c</sup>	40.12	-38.31	-126.25	117.56	-119.82	119.76
	Expt	32.75	-17.69	-121.74	120.76	-122.90	117.92
<b>Se(b)</b>	Opt <sup>a</sup>	40.62	-41.61	116.34	-119.76	127.89	-115.46
	Expt	34.57	-17.69	101.37	-138.23	129.99	-121.45

<sup>a</sup> NEVPT2. <sup>b</sup> B3LYP/6-31G(d,p). <sup>c</sup> B3LYP/ def2-SVP.

**Table S2.** Absolute NEVPT2 energies (Hartree), energy difference  $\Delta E_1$  (kcal/mol) between the different geometries for each complex, energy difference  $\Delta E_2$  (kcal/mol) of the two structures of  $\text{CoO}_2\text{Se}_2$ , and dipole moments  $\mu$  (Debye) of  $\text{CoO}_2\text{E}_2$ , E = S, Se complexes.

E atom	Geometry <sup>a</sup>	NEVPT2	$\Delta E_1$	$\Delta E_2$	M
S	Expt	-5671.628871			3.743
	B3LYP/6-31G(d,p)	-5673.160158	0.00		1.897
	B3LYP/def2-SVP	-5673.157838	1.46		1.852
Se (a)	Expt	-9761.619574			3.567
	B3LYP/6-31G(d,p)	-9763.427440	0.00		1.953
	B3LYP/def2-SVP	-9763.427335	0.07		2.245
Se (b)	Expt	-9761.545076		-46.75	5.463
	B3LYP/6-31G(d,p)	-9763.427822	-0.24	0.24	2.379

<sup>a</sup> Experimental crystal geometry or DFT optimized geometry.

**Table S3.** CASSCF vertical transition energies ( $T_e$  in eV) of the ground and the lowest excited states. All states are quartets. Their main electronic configurations ( $d_{xy} d_{yz} d_{z2} d_{xz} d_{x2-y2}$ ) of the  $\text{CoO}_2\text{E}_2$ , E = S, Se complexes.

				<b>E = S</b>		
<b>State</b>	<b><math>T_e</math></b>	<b>CASSCF<sup>a</sup></b>	<b><math>T_e</math></b>	<b>CASSCF<sup>b</sup></b>	<b><math>T_e</math></b>	<b>CASSCF<sup>c</sup></b>
0		0.43050 : 11212 0.39743 : 12112		0.37377 : 22111 0.23078 : 21211	0	0.46968 : 21211 0.29823 : 22111
1	0.215	0.48085 : 11212 0.34692 : 12112	0.210	0.50733 : 21211 0.16167 : 11212	0.273	0.22058 : 22111 0.19031 : 11212
2	0.441	0.45467 : 21211 0.30983 : 22111	0.429	0.32872 : 12112 0.26958 : 11212	0.407	0.32790 : 11212 0.31783 : 12112
3	0.493	0.38035 : 11122 0.31897 : 12121	0.470	0.40586 : 21121 0.31801 : 12121	0.467	0.53844 : 21121 0.13863 : 21211
4	0.618	0.35079 : 21211 0.20131 : 12121 0.19318 : 22111	0.603	0.44004 : 11212 0.16347 : 12121	0.635	0.29233 : 12121 0.23849 : 11212 0.21287 : 12112
5	0.659	0.25175 : 11221 0.23933 : 11122 0.18106 : 22111	0.633	0.18341 : 11221 0.17050 : 11122	0.671	0.49809 : 11122 0.25717 : 11221
6	0.754	0.61237 : 21121 0.21331 : 12211	0.722	0.49372 : 11122 0.14963 : 22111	0.721	0.25955 : 22111 0.17388 : 11212
0	<b><math>q_{\text{Co}}^d</math></b>	6.30/12.47/7.14		6.30/12.46/7.14		6.34 /12.50/7.16
				<b>E = Se (a)</b>		
<b>State</b>	<b><math>T_e</math></b>	<b>CASSCF<sup>a</sup></b>	<b><math>T_e</math></b>	<b>CASSCF<sup>b</sup></b>	<b><math>T_e</math></b>	<b>CASSCF<sup>c</sup></b>
0		0.68792 : 11212 0.14835 : 12112		0.40854 : 22111 0.20608 : 21211	eV	0.40411 : 21211 0.38083 : 22111
1	0.249	0.45761 : 12112 0.23778 : 11212	0.198	0.54960 : 21211 0.14122 : 11212	0.256	0.23604 : 21211 0.19969 : 12121
2	0.412	0.60391 : 11122 0.11603 : 11221	0.399	0.34171 : 12112 0.25635 : 11212	0.394	0.36321 : 12112 0.33047 : 11212 0.19907 : 12211
3	0.483	0.68381 : 21211 0.10331 : 21121	0.457	0.41133 : 21121 0.30010 : 12121	0.453	0.56755 : 21121 0.13565 : 21211
4	0.621	0.51661 : 12121 0.14423 : 21112	0.566	0.46521 : 11212 0.15189 : 12121 0.15119 : 12112	0.606	0.28630 : 11122 0.18050 : 11212
5	0.677	0.46463 : 22111 0.15894 : 11221	0.613	0.17941 : 11221 0.17326 : 11122 0.14843 : 22111	0.638	0.34618 : 11122 0.20838 : 11221
6	0.724	0.57002 : 21121 0.15460 : 12211	0.692	0.47317 : 11122 0.14904 : 22111	0.698	0.24235 : 11212 0.22701 : 22111
0	<b><math>q_{\text{Co}}^d</math></b>	6.31/12.51/7.14		6.31/12.47/7.13		6.34/12.50/7.14
				<b>E = Se (b)</b>		
<b>State</b>	<b><math>T_e</math></b>	<b>CASSCF<sup>a</sup></b>	<b><math>T_e</math></b>	<b>CASSCF<sup>c</sup></b>		
0		0.86280 : 11212		0.55375 : 21211 0.10906 : 11212		
1	0.228	0.61718 : 12112	0.220	0.35664 : 22111		

		0.17582 : 12211		0.21846 : 11212			
2	0.435	0.81664 : 21211	0.380	0.21821 : 12121 0.19120 : 21121 0.16918 : 12211			
3	0.462	0.66981 : 11122 0.14432 : 11221	0.409	0.42129 : 11212 0.25562 : 21121 0.16232 : 12112			
4	0.621	0.54440 : 22111 0.16590 : 11221	0.503	0.28535 : 12112 0.23695 : 22111 0.14335 : 11212			
5	0.644	0.65356 : 12121 0.20634 : 21112	0.601	0.51278 : 12121 0.17978 : 21112			
6	0.744	0.57376 : 21121 0.17479 : 12211	0.778	0.55010 : 11122 0.20301 : 11221			
0	<b>q<sub>Co</sub><sup>d</sup></b>	6.31/12.51/7.13		6.36/12.53/7.15			

<sup>a</sup> NEVPT2/ZORA-def2-TZVP<sub>Co,Se,S,O</sub> ZORA-def2-SVP<sub>P,N,C,H</sub> // B3LYP/6-31G(d,p).

<sup>b</sup> NEVPT2/ZORA-def2-TZVP<sub>Co,Se,S,O</sub> ZORA-def2-SVP<sub>P,N,C,H</sub> // B3LYP/def2-SVP.

<sup>c</sup> NEVPT2/ZORA-def2-TZVP<sub>Co,Se,S,O</sub> ZORA-def2-SVP<sub>P,N,C,H</sub> // Experimental crystal geometries, Refs. 1, 2.

<sup>d</sup> Total Mulliken charges on s / p / d orbitals of Co.

**Table S4.** NEVPT2-LFT  $d$ -orbital splitting and corresponding field matrix.

<b>E = S</b>								
NEVPT2 <sup>a</sup>	Orbital	Energy (eV)	Energy (cm <sup>-1</sup> )	$d_{xy}$	$d_{yz}$	$d_{z2}$	$d_{xz}$	$d_{x2-y2}$
	1	0.000	0.0	0.173163	0.050797	-0.541521	-0.068990	0.818187
	2	0.043	343.5	0.169875	0.714354	-0.523146	-0.044621	-0.430312
	3	0.244	1968.5	-0.044741	0.650274	0.543282	0.386613	0.361270
	4	0.483	3898.3	-0.889789	0.187289	-0.075686	-0.398524	0.092992
	5	0.565	4556.3	-0.383966	-0.170834	-0.363579	0.827622	-0.078981
NEVPT2 <sup>b</sup>	Orbital	Energy (eV)	Energy (cm <sup>-1</sup> )	$d_{xy}$	$d_{yz}$	$d_{z2}$	$d_{xz}$	$d_{x2-y2}$
	1	0.000	0.0	-0.751374	-0.199037	0.558918	-0.063882	-0.281694
	2	0.037	299.0	0.339035	-0.772693	0.351194	0.303190	0.269703
	3	0.232	1870.6	0.214342	0.553688	0.692439	0.004746	0.409869
	4	0.473	3814.9	-0.360013	-0.164674	-0.208153	-0.458899	0.767696
	5	0.535	4317.2	0.380712	-0.172165	0.203653	-0.832697	-0.300930
NEVPT2 <sup>c</sup>	Orbital	Energy (eV)	Energy (cm <sup>-1</sup> )	$d_{xy}$	$d_{yz}$	$d_{z2}$	$d_{xz}$	$d_{x2-y2}$
	1	0.000	0.0	-0.764756	-0.201070	0.468683	-0.329479	-0.215636
	2	0.062	503.8	0.449559	-0.641220	0.584329	0.042575	0.208521
	3	0.338	2722.2	0.031900	0.535562	0.345520	-0.356125	0.682602
	4	0.452	3646.4	-0.187188	-0.508724	-0.563110	-0.379875	0.494735
	5	0.551	4444.2	0.420700	0.052734	-0.049183	-0.786448	-0.446443
	<b>E = Se (a)</b>							
NEVPT2 <sup>a</sup>	Orbital	Energy (eV)	Energy (cm <sup>-1</sup> )	$d_{xy}$	$d_{yz}$	$d_{z2}$	$d_{xz}$	$d_{x2-y2}$
	1	0.000	0.0	-0.218962	-0.159054	-0.702418	0.290026	0.590975
	2	0.086	692.5	0.082405	-0.453485	-0.445485	0.227976	-0.732892
	3	0.313	2524.5	0.297217	-0.660787	0.469413	0.415620	0.286242
	4	0.508	4095.0	-0.022444	0.529635	0.111385	0.828818	-0.140132
	5	0.589	4753.3	-0.925432	-0.227815	0.274585	0.065060	-0.109758
NEVPT2 <sup>b</sup>	Orbital	Energy (eV)	Energy (cm <sup>-1</sup> )	$d_{xy}$	$d_{yz}$	$d_{z2}$	$d_{xz}$	$d_{x2-y2}$
	1	0.000	0.0	-0.761544	-0.235812	0.558966	-0.061256	-0.219655
	2	0.044	354.3	0.351416	-0.782672	0.292116	0.320044	0.275991
	3	0.218	1759.7	0.216733	0.532656	0.694770	0.061819	0.427525
	4	0.450	3628.9	-0.307497	-0.145325	-0.227714	-0.479373	0.776320
	5	0.539	4347.2	0.393738	-0.164243	0.260127	-0.812526	-0.300216
NEVPT2 <sup>c</sup>	Orbital	Energy (eV)	Energy (cm <sup>-1</sup> )	$d_{xy}$	$d_{yz}$	$d_{z2}$	$d_{xz}$	$d_{x2-y2}$
	1	0.000	0.0	-0.580000	-0.442569	0.584087	-0.355345	-0.017490
	2	0.044	351.1	0.672792	-0.579136	0.362494	0.209567	0.191394
	3	0.306	2470.2	0.155744	0.568781	0.443989	-0.263380	0.621077
	4	0.443	3569.8	-0.053030	-0.376815	-0.574624	-0.417792	0.591992
	5	0.542	4372.6	0.428815	0.056859	-0.011039	-0.765436	-0.476310
	<b>E = Se (b)</b>							
NEVPT2 <sup>a</sup>	Orbital	Energy (eV)	Energy (cm <sup>-1</sup> )	$d_{xy}$	$d_{yz}$	$d_{z2}$	$d_{xz}$	$d_{x2-y2}$
	1	0.000	0.0	-0.092062	-0.018978	-0.509507	0.171141	0.838020
	2	0.090	722.6	-0.122544	-0.322937	-0.753837	0.203383	-0.520635
	3	0.301	2426.6	0.137845	-0.804626	0.355295	0.438301	0.123427
	4	0.501	4037.3	0.977706	0.050932	-0.196081	-0.055216	0.000622
	5	0.564	4546.6	0.039968	0.495313	0.086319	0.856849	-0.106897
NEVPT2 <sup>c</sup>	Orbital	Energy (eV)	Energy (cm <sup>-1</sup> )	$d_{xy}$	$d_{yz}$	$d_{z2}$	$d_{xz}$	$d_{x2-y2}$
	1	0.000	0.0	-0.767682	0.306703	0.355474	0.077618	-0.429199
	2	0.098	788.4	0.245310	-0.560062	0.757568	0.129923	-0.188054
	3	0.354	2853.3	-0.220855	-0.637196	-0.541537	0.123793	-0.486434

	4	0.439	3537.4	-0.449034	-0.395916	0.079755	-0.643803	0.469867
	5	0.597	4812.1	0.316353	0.171742	0.010316	-0.739789	-0.568358

<sup>a</sup> NEVPT2-LFT/ZORA-def2-TZVP<sub>Co,Se,S,O</sub>ZORA-def2-SVP<sub>P,N,C,H</sub> // B3LYP/6-31G(d,p).

<sup>b</sup> NEVPT2-LFT/ZORA-def2-TZVP<sub>Co,Se,S,O</sub>ZORA-def2-SVP<sub>P,N,C,H</sub> //B3LYP/def2-SVP.

<sup>c</sup> NEVPT2-LFT/ZORA-def2-TZVP<sub>Co,Se,S,O</sub>ZORA-def2-SVP<sub>P,N,C,H</sub> // Experimental crystal geometries, Refs. 1, 2.

**Table S5.** NEVPT2 vertical transition energies  $T_e$  (eV) and state contribution to zfs parameters for the calculated states of the  $\text{CoO}_2\text{E}_2$ , E = S, Se complexes.

GS	s <sup>c</sup>	E = S												$T_e$			$T_e^a$			$D$			$E$				
		$T_e$			$T_e^a$			$D$			$E$			$T_e$			$T_e^a$			$D$			$E$				
		NEVPT2 <sup>b</sup>			NEVPT2 <sup>c</sup>			NEVPT2 <sup>c</sup>			NEVPT2 <sup>d</sup>			NEVPT2 <sup>d</sup>			NEVPT2 <sup>d</sup>			NEVPT2 <sup>d</sup>			NEVPT2 <sup>d</sup>				
GS	s <sup>c</sup>	0.000	0.000	0.00	0.00	0.000	0.000	0.00	0.00	0.00	0.000	0.000	0.00	0.000	0.000	0.00	0.000	0.000	0.00	0.000	0.000	0.00	0.000	0.000	0.00		
1	4	0.275	0.225	26.30	25.84	0.270	0.217	27.03	26.47	0.355	0.286	20.94	20.20														
2	4	0.586	0.457	-23.86	-0.09	0.570	0.442	-24.59	-0.08	0.544	0.423	-19.85	-0.88														
3	4	0.647	0.504	9.77	-9.28	0.617	0.477	10.27	-9.51	0.619	0.484	6.62	-8.59														
4	4	0.830	0.645	0.05	0.05	0.808	0.625	0.05	0.05	0.830	0.664	-0.08	-0.08														
5	4	0.861	0.681	-0.03	0.00	0.830	0.650	-0.03	0.00	0.872	0.701	0.02	0.00														
6	4	0.961	0.770	0.15	-0.07	0.926	0.733	0.13	-0.05	0.967	0.748	-0.05	0.01														
7	4	2.256	2.188	0.00	0.00	2.235	2.166	0.00	0.00	2.241	2.178	0.00	0.00														
8	4	2.444	2.335	0.00	0.00	2.434	2.324	0.00	0.00	2.479	2.349	0.00	0.00														
9	4	2.631	2.481	0.00	0.00	2.615	2.466	0.00	0.00	2.566	2.433	0.00	0.00														
0	2	2.233	2.128	0.68	0.01	2.251	2.140	0.63	0.00	2.262	2.148	-0.06	0.03														
1	2	2.271	2.156	0.00	0.00	2.274	2.158	0.00	0.00	2.286	2.156	0.13	0.03														
2	2	2.303	2.208	-0.05	0.01	2.306	2.207	-0.02	0.00	2.300	2.200	0.03	0.00														
3	2	2.309	2.198	-0.13	0.12	2.315	2.202	-0.16	0.16	2.316	2.221	0.06	0.05														
4	2	2.353	2.233	0.02	0.00	2.359	2.237	0.02	0.00	2.351	2.234	-0.02	0.01														
5	2	2.421	2.301	0.06	0.00	2.419	2.296	0.05	0.00	2.460	2.322	0.00	0.00														
6	2	2.546	2.369	-3.20	-2.89	2.543	2.364	-3.18	-2.82	2.595	2.399	-2.94	-2.45														
7	2	2.734	2.492	-0.07	1.78	2.716	2.477	-1.55	2.32	2.688	2.462	3.27	0.77														
8	2	2.742	2.497	2.19	0.99	2.724	2.483	3.65	0.48	2.727	2.484	-0.40	1.86														
9	2	2.797	2.740	0.00	0.00	2.794	2.739	0.00	0.00	2.821	2.758	-0.01	0.00														
10	2	2.923	2.801	0.00	0.00	2.920	2.800	0.00	0.00	2.967	2.826	0.00	0.00														
11	2	2.991	2.842	-0.26	-0.22	2.984	2.837	-0.24	-0.21	2.983	2.854	-0.06	-0.07														
12	2	3.035	2.871	-0.14	0.04	3.029	2.860	-0.15	0.03	3.062	2.881	-0.23	-0.23														
13	2	3.143	2.951	0.47	0.00	3.138	2.979	0.48	0.00	3.084	2.887	0.29	0.02														
14	2	3.154	2.989	-0.09	0.00	3.141	2.942	-0.09	0.00	3.094	2.898	-0.08	0.11														
15	2	3.174	2.957	-0.01	0.00	3.167	2.948	0.00	0.00	3.152	3.013	0.06	0.02														
16	2	3.298	3.180	0.01	0.00	3.272	3.162	0.08	0.00	3.318	3.178	-0.01	-0.01														
17	2	3.324	3.165	0.00	0.02	3.308	3.147	-0.07	0.03	3.328	3.146	0.01	0.00														
18	2	3.376	3.173	0.00	0.00	3.352	3.155	0.00	0.00	3.350	3.165	-0.01	0.01														
19	2	3.397	3.134	-0.03	0.02	3.357	3.116	-0.02	0.02	3.361	3.125	0.02	0.00														
20	2	3.409	3.141	-0.05	0.06	3.411	3.122	-0.05	0.05	3.369	3.112	-0.03	0.03														
21	2	3.536	3.295	0.06	0.01	3.515	3.275	0.05	0.01	3.489	3.237	0.05	0.07														
22	2	3.609	3.390	-0.39	0.28	3.570	3.366	-0.32	0.21	3.577	3.362	0.10	0.07														
23	2	3.621	3.378	-0.02	0.40	3.599	3.359	-0.44	0.53	3.613	3.386	-0.49	0.60														
24	2	3.631	3.340	1.09	0.08	3.618	3.323	1.50	0.02	3.628	3.306	0.85	-0.01														
25	2	3.762	3.496	-0.35	-0.31	3.726	3.469	-0.37	-0.34	3.723	3.467	-0.38	-0.37														
26	2	3.870	3.582	0.00	0.00	3.834	3.553	0.00	0.00	3.873	3.575	0.00	0.00														
27	2	3.942	3.634	0.00	0.00	3.899	3.599	0.00	0.00	3.947	3.631	0.01	0.00														
28	2	4.889	4.778	0.00	0.00	4.888	4.775	0.00	0.00	4.871	4.760	0.00	0.00														
29	2	4.930	4.787	-0.14	0.03	4.928	4.783	-0.14	0.04	4.932	4.780	-0.01	0.04														
30	2	5.033	4.864	0.25	0.00	5.032	4.862	0.25	0.00	4.996	4.828	0.16	0.03														
31	2	5.073	4.904	-0.12	-0.05	5.065	4.897	-0.12	-0.06	5.048	4.878	-0.14	-0.09														
32	2	5.160	4.959	-0.03	-0.01	5.152	4.951	-0.03	-0.01	5.125	4.926	-0.01	0.00														
33	2	5.165	4.969	0.02	0.00	5.156	4.961	0.02	0.00	5.133	4.935	0.00	0.00														

34	2	5.208	4.989	0.00	0.00	5.193	4.976	0.00	0.00	5.172	4.955	0.00	0.00
35	2	7.320	7.334	0.01	0.00	7.328	7.334	0.01	0.00	7.345	7.338	0.01	0.00
36	2	7.465	7.392	-0.01	0.00	7.463	7.392	-0.01	-0.01	7.389	7.349	-0.01	0.00
37	2	7.477	7.438	0.00	0.00	7.471	7.433	0.00	0.00	7.426	7.394	-0.01	-0.01
38	2	7.687	7.607	0.03	0.00	7.687	7.610	0.03	0.00	7.652	7.556	0.00	0.01
39	2	7.758	7.636	-0.03	0.02	7.761	7.639	-0.04	0.02	7.690	7.574	0.02	0.01

GS	s <sup>e</sup>	E = Se (a)											
		T <sub>e</sub>	T <sub>e</sub> <sup>a</sup>	D	E	T <sub>e</sub>	T <sub>e</sub> <sup>a</sup>	D	E	T <sub>e</sub>	T <sub>e</sub> <sup>a</sup>	D	E
NEVPT2 <sup>b</sup>				NEVPT2 <sup>c</sup>				NEVPT2 <sup>d</sup>					
		0.000	0.000	0.00	0.00	0.000	0.000	0.00	0.00	0.000	0.000	0.00	0.00
1	4	0.341	0.267	22.20	21.51	0.266	0.205	27.54	27.01	0.344	0.269	21.87	20.96
2	4	0.543	0.427	-12.34	-2.63	0.538	0.410	-25.77	-0.04	0.531	0.408	-23.51	-0.13
3	4	0.655	0.505	-1.01	-5.78	0.605	0.460	10.13	-9.39	0.601	0.467	9.36	-8.79
4	4	0.826	0.654	-0.13	-0.10	0.780	0.586	0.07	0.07	0.782	0.632	-0.01	-0.03
5	4	0.886	0.705	0.05	0.04	0.814	0.625	-0.05	0.00	0.855	0.665	0.02	-0.01
6	4	0.987	0.758	0.04	-0.05	0.892	0.701	0.21	-0.05	0.950	0.722	-0.04	0.00
7	4	2.200	2.135	0.00	0.00	2.203	2.130	0.01	0.00	2.193	2.131	0.00	0.00
8	4	2.473	2.350	0.00	0.00	2.404	2.291	0.00	0.00	2.471	2.332	0.00	0.00
9	4	2.636	2.478	0.00	0.00	2.623	2.466	0.01	0.00	2.576	2.440	0.00	0.00
0	2	2.243	2.135	0.03	0.02	2.242	2.123	0.67	0.00	2.252	2.137	-0.04	0.05
1	2	2.260	2.148	0.24	0.00	2.273	2.152	0.00	0.00	2.287	2.151	0.14	0.02
2	2	2.302	2.177	0.00	-0.02	2.309	2.191	-0.05	-0.01	2.289	2.190	-0.03	0.02
3	2	2.305	2.194	-0.19	0.21	2.317	2.205	-0.10	0.10	2.333	2.223	0.07	0.08
4	2	2.353	2.234	-0.04	0.00	2.384	2.283	0.01	0.00	2.335	2.219	-0.01	-0.02
5	2	2.428	2.299	0.00	0.00	2.393	2.236	0.08	0.00	2.444	2.304	0.01	0.00
6	2	2.590	2.386	-2.77	-2.28	2.540	2.351	-3.00	-2.65	2.583	2.382	-2.85	-2.22
7	2	2.691	2.458	0.55	1.74	2.693	2.451	-1.17	2.20	2.676	2.447	3.94	0.52
8	2	2.734	2.488	1.95	0.97	2.701	2.457	3.05	0.67	2.704	2.461	-1.30	2.15
9	2	2.769	2.713	-0.07	-0.06	2.797	2.732	0.00	0.00	2.805	2.740	-0.01	0.01
10	2	2.974	2.803	-0.004	0.01	2.874	2.764	-0.001	0.00	2.927	2.795	-0.012	-0.01
11	2	2.977	2.844	-0.056	0.01	2.982	2.824	-0.203	-0.15	2.964	2.826	-0.072	-0.08
12	2	3.066	2.882	0.180	-0.01	3.038	2.852	-0.106	0.06	3.061	2.867	-0.121	-0.08
13	2	3.087	2.904	-0.026	-0.15	3.124	2.974	-0.073	-0.06	3.090	2.892	-0.126	0.03
14	2	3.095	2.879	-0.044	0.08	3.140	2.921	0.347	0.01	3.102	2.882	0.279	-0.02
15	2	3.141	2.991	0.128	0.06	3.141	2.917	0.132	0.00	3.134	2.988	0.093	0.02
16	2	3.291	3.137	-0.013	-0.01	3.269	3.138	0.123	0.00	3.289	3.151	0.053	0.00
17	2	3.317	3.170	0.024	-0.01	3.280	3.119	-0.125	0.09	3.315	3.122	-0.015	-0.01
18	2	3.341	3.066	0.136	0.00	3.315	3.084	-0.001	0.00	3.324	3.081	0.016	0.01
19	2	3.380	3.119	-0.029	0.03	3.336	3.122	-0.045	0.04	3.335	3.136	-0.003	0.00
20	2	3.415	3.175	0.019	0.00	3.366	3.085	-0.065	0.06	3.336	3.093	-0.056	0.06
21	2	3.452	3.239	-0.086	0.14	3.498	3.256	0.073	0.01	3.445	3.217	0.008	0.10
22	2	3.602	3.357	0.177	-0.05	3.548	3.336	-0.314	0.14	3.571	3.335	0.169	0.12
23	2	3.613	3.372	-0.102	0.31	3.572	3.329	-0.581	0.56	3.577	3.276	-0.596	0.58
24	2	3.645	3.334	0.412	0.28	3.583	3.289	1.571	0.00	3.616	3.372	0.853	-0.06
25	2	3.756	3.475	-0.280	-0.29	3.695	3.432	-0.374	-0.33	3.694	3.432	-0.351	-0.37
26	2	3.874	3.565	-0.001	0.00	3.786	3.505	0.000	0.00	3.837	3.538	0.006	0.00
27	2	3.957	3.628	0.008	0.00	3.861	3.554	0.001	0.00	3.903	3.583	0.004	0.00
28	2	4.858	4.740	0.001	0.00	4.875	4.753	-0.001	0.00	4.858	4.740	-0.001	0.00

29	2	4.905	4.747	-0.017	0.06	4.914	4.761	-0.133	0.06	4.915	4.756	-0.066	0.06
30	2	5.003	4.837	0.079	-0.05	5.014	4.840	0.252	0.00	4.980	4.811	0.180	0.02
31	2	5.059	4.866	-0.026	-0.03	5.061	4.886	-0.107	-0.07	5.046	4.869	-0.108	-0.09
32	2	5.133	4.921	-0.012	-0.01	5.135	4.930	-0.035	-0.02	5.105	4.908	-0.030	-0.02
33	2	5.139	4.937	-0.017	-0.01	5.141	4.941	0.009	0.00	5.121	4.919	0.003	0.00
34	2	5.180	4.954	-0.009	-0.01	5.171	4.949	-0.004	0.00	5.154	4.934	0.000	0.00
35	2	7.304	7.301	0.007	0.00	7.316	7.304	0.011	0.00	7.306	7.286	0.006	0.00
36	2	7.311	7.272	-0.002	0.00	7.429	7.349	-0.013	-0.01	7.376	7.319	-0.008	-0.01
37	2	7.446	7.377	-0.009	-0.01	7.438	7.416	0.003	0.00	7.376	7.368	-0.002	0.00
38	2	7.632	7.554	0.012	0.01	7.686	7.603	0.030	0.00	7.650	7.559	0.027	0.00
39	2	7.749	7.613	-0.003	0.02	7.746	7.622	-0.033	0.03	7.701	7.577	-0.024	0.03

<b>E = Se (b)</b>													
GS	s <sup>e</sup>	T <sub>e</sub>	T <sub>e</sub> <sup>a</sup>	D	E	T <sub>e</sub>	T <sub>e</sub> <sup>a</sup>	D	E				
										NEVPT2 <sup>b</sup>			
								NEVPT2 <sup>d</sup>					
		0.000	0.000	0.000	0.00	0.000	0.000	0.000	0.00				
1	4	0.303	0.242	23.61	23.13	0.302	0.234	22.92	21.02				
2	4	0.592	0.458	-19.53	-0.86	0.527	0.397	-24.04	-0.15				
3	4	0.617	0.478	6.52	-8.67	0.580	0.434	8.02	-5.09				
4	4	0.847	0.673	0.03	0.02	0.678	0.530	-2.05	0.14				
5	4	0.854	0.655	-0.07	0.04	0.828	0.640	0.19	-0.20				
6	4	0.974	0.775	0.14	-0.06	1.080	0.838	-0.03	-0.03				
7	4	2.258	2.175	0.00	0.00	2.223	2.137	0.00	0.00				
8	4	2.419	2.304	0.00	0.00	2.387	2.287	0.00	0.00				
9	4	2.602	2.456	0.01	0.00	2.597	2.446	0.00	0.00				
0	2	2.243	2.123	0.40	0.03	2.135	2.054	-0.68	0.56				
1	2	2.265	2.145	-0.01	0.01	2.252	2.140	0.25	-0.01				
2	2	2.308	2.190	0.01	0.00	2.253	2.155	-0.03	-0.06				
3	2	2.314	2.205	-0.07	0.07	2.300	2.197	-0.17	-0.05				
4	2	2.346	2.228	-0.01	-0.02	2.364	2.232	-0.02	0.01				
5	2	2.434	2.305	0.04	-0.01	2.425	2.289	-0.03	0.01				
6	2	2.557	2.366	-3.00	-2.64	2.535	2.341	-2.40	-1.31				
7	2	2.711	2.467	-1.75	2.36	2.641	2.420	4.12	0.12				
8	2	2.726	2.479	3.78	0.47	2.690	2.441	-2.51	2.04				
9	2	2.798	2.744	0.02	0.00	2.776	2.740	-0.02	-0.08				
10	2	2.941	2.806	-0.007	-0.01	2.934	2.801	-0.053	-0.05				
11	2	3.004	2.846	-0.173	-0.12	2.937	2.825	0.285	-0.04				
12	2	3.036	2.866	-0.107	0.05	3.066	2.870	-0.025	-0.07				
13	2	3.106	2.890	-0.011	-0.07	3.088	2.872	-0.118	0.00				
14	2	3.108	2.903	0.164	0.02	3.137	2.920	0.069	0.04				
15	2	3.134	2.993	0.140	0.00	3.205	2.976	-0.029	-0.03				
16	2	3.310	3.149	0.046	0.00	3.237	3.024	0.329	0.00				
17	2	3.327	3.134	-0.052	0.04	3.281	3.065	0.019	0.05				
18	2	3.331	3.173	0.020	0.01	3.333	3.091	-0.048	0.00				
19	2	3.354	3.104	-0.096	0.10	3.342	3.138	0.022	0.00				
20	2	3.425	3.119	-0.031	0.04	3.380	3.177	0.003	0.00				
21	2	3.494	3.255	0.068	0.02	3.513	3.238	0.000	0.01				
22	2	3.568	3.355	-0.122	0.02	3.536	3.302	-0.039	0.23				
23	2	3.578	3.354	-0.590	0.56	3.560	3.287	-0.590	0.65				

24	2	3.655	3.319	1.445	0.01	3.593	3.364	0.829	-0.12
25	2	3.764	3.482	-0.350	-0.28	3.741	3.449	-0.150	-0.30
26	2	3.847	3.551	0.000	0.00	3.784	3.499	-0.002	-0.02
27	2	3.958	3.628	0.005	0.00	3.896	3.574	0.012	-0.01
28	2	4.864	4.742	-0.001	0.00	4.874	4.740	-0.001	0.00
29	2	4.914	4.753	-0.125	0.06	4.915	4.747	-0.051	0.07
30	2	5.004	4.825	0.255	0.00	4.987	4.817	0.078	-0.01
31	2	5.033	4.864	-0.125	-0.07	5.029	4.855	0.034	-0.07
32	2	5.121	4.913	-0.011	-0.01	5.078	4.888	-0.026	-0.03
33	2	5.124	4.923	0.000	0.00	5.089	4.908	-0.009	-0.01
34	2	5.175	4.947	0.000	0.00	5.149	4.928	0.001	0.00
35	2	7.327	7.302	0.009	0.00	7.349	7.285	0.005	0.00
36	2	7.400	7.339	-0.007	-0.01	7.388	7.324	-0.006	-0.01
37	2	7.413	7.375	-0.006	-0.01	7.411	7.387	-0.003	0.00
38	2	7.622	7.540	0.030	0.00	7.561	7.521	0.031	0.00
39	2	7.675	7.560	-0.030	0.03	7.700	7.577	-0.048	0.05

<sup>a</sup> NEVPT2-LFT

<sup>b</sup> NEVPT2/ZORA-def2-TZVP<sub>Co,Se,S,O</sub>ZORA-def2-SVP<sub>P,N,C,H</sub> // B3LYP/6-31G(d,p).

<sup>c</sup> NEVPT2/ZORA-def2-TZVP<sub>Co,Se,S,O</sub>ZORA-def2-SVP<sub>P,N,C,H</sub> //B3LYP/def2-SVP.

<sup>d</sup> NEVPT2/ZORA-def2-TZVP<sub>Co,Se,S,O</sub>ZORA-def2-SVP<sub>P,N,C,H</sub> // Experimental crystal geometries, Refs. 1, 2.

<sup>e</sup> s: Multiplicity of spin 2S+1.

## References

1. M. C. Aragoni, M. Arca, M. B. Carrea, A. Garau, F. A. Devillanova, F. Isaia, V. Lippolis, G. L. Abbati, F. Demartin, C. Silvestru, S. Demeshko and F. Meyer, *Eur. J. Inorg. Chem.*, 2007, 4607-4614.
2. E. Ferentinos, D. Maganas, C. P. Raptopoulou, A. Terzis, V. Pscharis, N. Robertson and P. Kyritsis, *Dalton Trans.*, 2011, **40**, 169-180.
3. J. Nehrkorn, J. Telser, K. Holldack, S. Stoll and A. Schnegg, *J. Phys. Chem. B*, 2015, **119**, 13816-13824.